5-1-2004

Geometry Analysis of an Inverse-Geometry Volumetric CT System With Multiple Detector Arrays

Samuel R. Mazin
Stanford University

Taly Gilat Schmidt
Marquette University, tal.gilat-schmidt@marquette.edu

Edward G. Solomon
NexRay, Inc.

Rebecca Fahrig
Stanford University

Norbert J. Pelc
Stanford University

Geometry analysis of an inverse-geometry volumetric CT system with multiple detector arrays

Samuel Mazin[a,b], Taly Gilat Schmidt[a,b], Edward Solomon[c], Rebecca Fahrig[a], Norbert Pelc[a]

[a]Department of Radiology, Stanford University, Stanford, CA 94305
[b]Department of Electrical Engineering, Stanford University, Stanford, CA 94305
[c]NexRay Inc., Los Gatos, CA 95032

ABSTRACT

An inverse-geometry volumetric CT (IGCT) system for imaging in a single fast rotation without cone-beam artifacts is being developed. It employs a large scanned source array and a smaller detector array. For a single-source/single-detector implementation, the FOV is limited to a fraction of the source size. Here we explore options to increase the FOV without increasing the source size by using multiple detectors spaced apart laterally to increase the range of radial distances sampled. We also look at multiple source array systems for faster scans. To properly reconstruct the FOV, Radon space must be sufficiently covered and sampled in a uniform manner. Optimal placement of the detectors relative to the source was determined analytically given system constraints (5cm detector width, 25cm source width, 45cm source-to-isocenter distance). For a 1x3 system (three detectors per source) detector spacing (DS) was 18° and source-to-detector distances (SDD) were 113, 100 and 113cm to provide optimum Radon sampling and a FOV of 44cm. For multiple-source systems, maximum angular spacing between sources cannot exceed 125° since detectors corresponding to one source cannot be occluded by a second source. Therefore, for 2x3 and 3x3 systems using the above DS and SDD, optimum spacing between sources is 115° and 61° respectively, requiring minimum scan rotations of 115° and 107°. Also, a 3x3 system can be much faster for full 360° dataset scans than a 2x3 system (120° vs. 245°). We found that a significantly increased FOV can be achieved while maintaining uniform radial sampling as well as a substantial reduction in scan time using several different geometries. Further multi-parameter optimization is underway.

Keywords: Volumetric CT, VCT, CT geometry, inverse-geometry CT, IGCT

1. INTRODUCTION

An inverse-geometry volumetric CT (IGCT) system has been proposed recently.[1] It consists of a large scanned source array coupled with a fast small detector array. The aim is to reconstruct a volume in a single rotation with negligible cone-beam artifacts that arise in traditional cone-beam tomography systems.[2] Figure 1(a) is a depiction of this system.

Although the source array and detector array have the same axial extent, the source array is much larger than the detector array in the in-plane direction. Thus in-plane projections are fan-like and the system needs only a single rotation to acquire a complete dataset for all axial planes. In addition, rays that cross through the plane of interest at an angle (i.e. rays that are not in-plane) may be used for reconstruction.

Since the source array is much larger than the detector array, the in-plane field-of-view (FOV) is determined mostly by the in-plane (transverse) extent of the source array as can be seen in Fig. 1(b). However, if more small detector arrays are added to the system (each with the same axial extent as the source array), the FOV increases substantially without changing the source size. For example, if instead of one small detector array there are three detector arrays, spaced apart properly, then the FOV increases by about a factor of three as can be seen in Fig. 1(c).

Further, to reduce scan time, more source/multi-detector pairs can be added so that more projection data may be acquired simultaneously.

1.1. Increasing the FOV

The primary objective is to increase the FOV in the transverse direction, by adding more small detector arrays. It is also desirable to keep a relatively uniform sampling of rays that are equidistant from the FOV center.

Medical Imaging 2004: Physics of Medical Imaging, edited by Martin J. Yaffe, Michael J. Flynn, Proceedings of SPIE Vol. 5368 (SPIE, Bellingham, WA, 2004) · 1605-7422/04/$15 · doi: 10.1117/12.536032

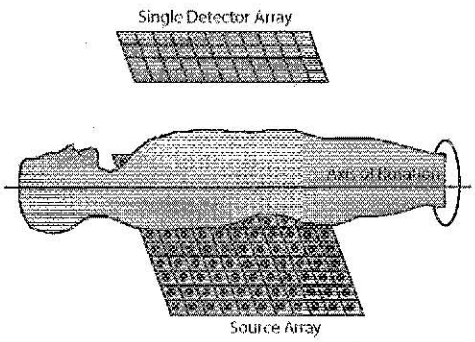

(a) 3-D view of an IGCT system with a single detector array.

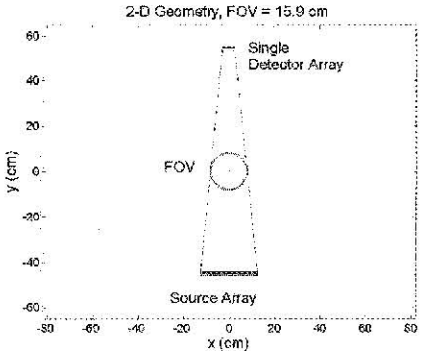

(b) Transverse view of an IGCT system with a single detector array.

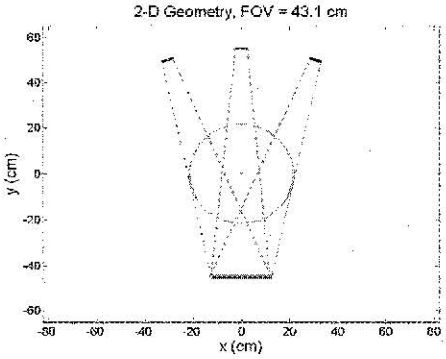

(c) Transverse view of an IGCT system with three detector arrays.

Figure 1. IGCT system with a single detector array (3-D and transverse views) and transverse view of a system with three detector arrays with a three-fold increase in the field-of-view.

1.2. Reducing scan time

The secondary objective is to reduce the scan time. Because a source/multi-detector pair does not fully surround the object, one can envision adding additional source/multi-detector pairs that do not overlap so that the CT acquisition may be done in a more parallel fashion. This would significantly reduce both the full and partial-scan times.

This study is an analysis of an IGCT system with multiple detector arrays with emphasis on increasing FOV and reducing scan time.

2. SYSTEM GEOMETRY

We define the z-axis to be the axis of rotation of the system. The z-axis is also referred to as the axial direction. A transverse direction is any direction perpendicular to the axial direction. Thus a transverse plane is a cut through the system perpendicular to the axis of rotation.

The base system consists of a flat scanned-anode x-ray source array opposite multiple flat detector arrays that are much smaller in the transverse direction but are of the same axial extent as the source array. The lengths of the source and detector arrays are parallel to the z-axis and the widths are their extents in the transverse plane. Because the FOV in the axial direction depends only on the axial extent of the source and detector arrays, we model the IGCT system strictly in the transverse plane to simplify the analysis. From now on, FOV will refer to the transverse FOV.

We model the source array in the transverse view as a line parallel to the horizontal x-axis. The detector arrays are also modeled as lines and are situated across from the source array. Each detector array is perpendicular to the line connecting its center to the center of the source array.

2.1. System Parameters

We consider a system with three detector arrays consisting of one central array and two placed symmetrically on either side (Fig. 2). A system with only two detector arrays (with the same dimensions) does not lead to a significant enough increase in the FOV. We define O to be the isocenter (axis of rotation) and S to be the point defining the center of the source array. Let D_C be the center of the central detector array and D_R be the center of the right-most detector array. Let SDD_C be the source-to-detector-distance from S to D_C and let SDD_R be the distance from S to D_R. Let SID, the source-to-isocenter-distance, be the distance from S to O. To characterize the angular position of the outer detectors relative to the source we let α be the angle between the lines SD_C and SD_R. Note that the three detector array positions are fully characterized by the parameters SDD_C, SDD_R and α.

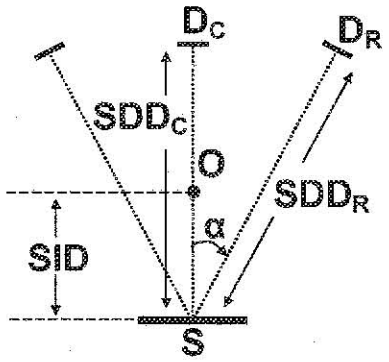

Figure 2. System with three detector arrays outlining the main parameters characterizing the system geometry.

For this study, values for the parameters listed in Table 1 were fixed while α and SDD_R were considered to be the free parameters. The goal was to select the values of α and SDD_R that optimized the uniformity of radial sampling in Radon space as described below.

Table 1. Specifications for IGCT system with three detector arrays.

SDD_C	100 cm
SID	45 cm
Source array width	25 cm
Detector array widths	5 cm
Source array spot spacing	0.25 cm
Detector array element spacing	0.1 cm

3. UNIFORM SAMPLING IN RADON SPACE

As shown in Fig. 3 the FOV in the IGCT system increases as the detector arrays are moved farther apart. However, if the detector arrays are moved too far apart, then one can see that portions within the FOV will be undersampled relative to others. Thus there is a balance between FOV size and uniform sampling within the FOV.

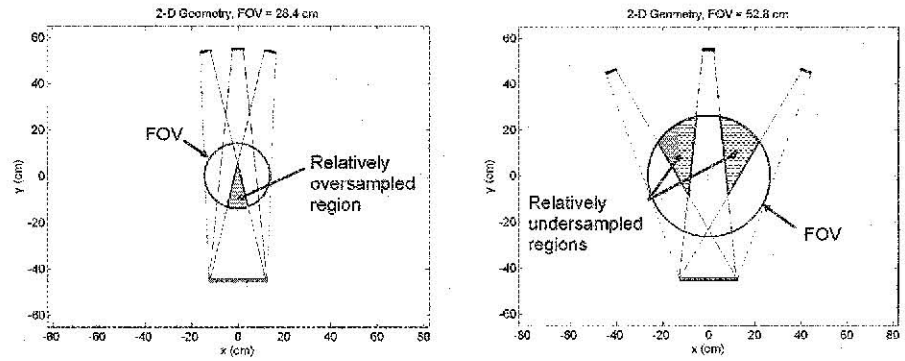

(a) Small detector array spacing yields smaller FOV with relatively oversampled regions.

(b) Large detector array spacing yields larger FOV with relatively undersampled regions.

Figure 3. Detector array spacing results in a tradeoff between FOV size and over/undersampled regions in FOV.

It is helpful to look at the problem in Radon space. Consider Fig. 4. We characterize each ray by two parameters (ρ, θ): ρ is the signed distance between the ray and the isocenter, and θ is the angle between the horizontal x-axis and the ray's perpendicular line to the isocenter. Because ρ is signed we have $\rho \in [-\frac{FOV}{2}, \frac{FOV}{2}]$ and $\theta \in [-\frac{\pi}{2}, \frac{\pi}{2}]$.

We now need a mapping between a general ray and its point in Radon space (ρ, θ). Let the ray origin be R_S and the ray destination at the detector be R_D. Let s be the signed distance from the source midpoint to R_S and d be the signed distance from the detector midpoint to R_D. That is, s is the displacement of the ray origin from the source center and d is the displacement from the center of the corresponding detector array. Then from basic geometry we have the following mapping equations:

$$\theta = \arctan\{\frac{s\cos(\alpha) - d}{SDD\cos(\alpha) - d\sin(\alpha)} - \tan(\alpha)\} \tag{1}$$

$$\rho = d\cos(\alpha + \theta) + SDD\sin(\alpha + \theta) - SID\{\cos(\theta)\tan(\alpha + \theta) - \frac{\sin(\alpha)}{\cos(\alpha + \theta)}\} \tag{2}$$

Where, again, α is the angular displacement of the detector array hit by the ray ($\alpha = 0$ for the central detector array), and SDD is the distance between the source and the the detector array (for our purposes $SDD = SDD_C$ or SDD_R).

Since every ray represents a point in Radon space, we can look at the coverage in Radon space of a system with three detector arrays at a single angular position of the gantry. Figure 5(a) shows this for $\alpha = 20^o$ and $SDD_R = 113$cm. The horizontal axis is the signed distance ρ, the vertical axis is the ray angle θ. Each detector array contributes points in Radon space that fall inside a polygon that resembles a parallelogram. The central polygon in the figure represents the contribution from the central detector array. The length of the long axis of

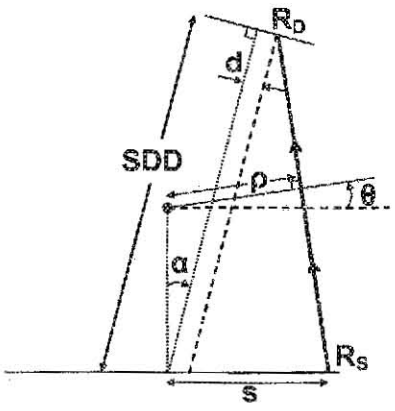

Figure 4. Relationship between a ray's Cartesian parameters and its Radon space parameters (ρ, θ). The figure is for illustration purposes and is not to scale.

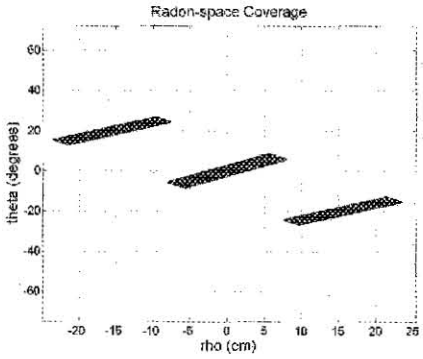

(a) Radon space coverage for a system with three detector arrays. Each detector array contributes samples to one of the polygons.

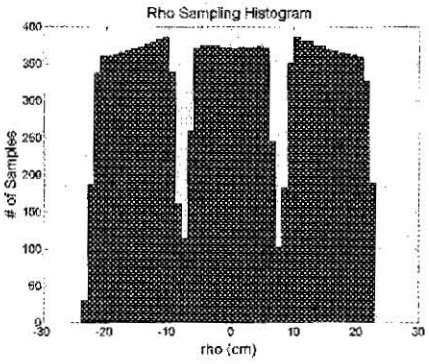

(b) ρ sampling histogram that shows undersampled areas in the FOV. Note that the outer detector arrays intrinsically have a non-uniform sampling density (the histogram slopes in these areas).

Figure 5. Radon space analysis for a system with three detectors that are spaced to widely apart. Although the FOV is large, undersampling of some areas in the FOV can be seen.

the polygon is determined by the width of the source array while the shorter axis is determined by the width of the detector array. We can now easily see how adding more detector arrays can significantly increase the FOV.

Figure 5(b) shows a histogram of the number of samples per unit ρ which is simply a vertical integration of Fig. 5(a). From this graph it is clear that some ρ distances are undersampled. If the detector arrays are brought too close together, the parallelograms in Fig. 5(a) move closer together and we will have oversampled regions where they overlap at the expense of FOV size. Therefore we would like the histogram to be relatively flat to achieve a uniform sampling in Radon space while maximizing the FOV. Note that we cannot achieve a perfectly flat histogram because the outer detector arrays have an intrinsic non-uniform sampling property: rays closer to the isocenter (smaller ρ distances) are sampled more densely since θ changes more slowly for those rays.

3.1. Choosing the Detector Positions

Since we are dealing with three detector arrays, and we are leaving the central detector array distance SDD_C fixed, we have α and SDD_R as two free parameters to vary to achieve the goal of maximizing the FOV while maintaining a ρ-uniform sampling in Radon space.

If we force SDD_R (representing both outer detector array distances due to symmetry) to be fixed and are allowed to vary α, then the Radon space polygons move relative to each other. Since we wish the resulting ρ sampling histogram to be uniform we would like to overlap the polygons so that the vertical integration is relatively constant over ρ (neglecting the FOV edge areas where ρ is close to $\pm\frac{FOV}{2}$). Since the left and right detector array positions should be symmetric, we focus on the central and right detector arrays. Intuitively, α should be chosen so that as ρ increases to the edge of the sampling provided by the central detector, the right detector's FOV sampling will compensate. Thus we want to choose α so that the midpoints of the short sides of their Radon space polygons are aligned at the same ρ position. Let S_L and S_R denote the left and right ends of the source array. Then these midpoints correspond to the rays $S_R D_C$ and $S_L D_R$ (see Fig. 6).

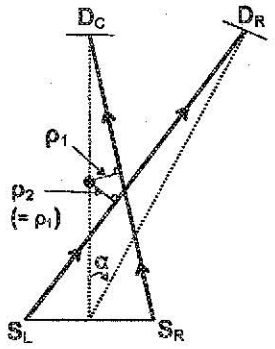

Figure 6. α is chosen so that the two rays shown have the same ρ distance. Intuitively, the right detector picks up at the same ρ at which that the center detector ends.

Since the correct α results in these rays having the same ρ value, Eqns. 1 and 2 must be solved in α for both rays where $\rho_1 = \rho_2$, $d_1 - d_2 = 0$, $s_1 = -s_2 = |S_R - S|$, $SDD_1 = SDD_C$, $SDD_2 = SDD_R$, $\alpha_1 = 0$, and $\alpha_2 = \alpha$.

We now examine the problem of choosing the best SDD_R keeping α fixed. Increasing SDD_R means that the outer detector arrays move outward away from the source and thus the FOV of the outer detector arrays increase slightly. Because the central and outer detectors are assumed to have the same number of detector elements, with an approximately equal $\Delta\theta$ between neighboring ray measurements, ρ-uniform sampling is achieved when their respective FOV sizes are equal (i.e. when each detector "sees" the same amount of the total FOV). We can again use Eqns. 1 and 2 to solve for SDD_R given α so that $FOV_1 = \rho_{1,MAX} - \rho_{1,MIN} = \rho_{2,MAX} - \rho_{2,MIN} = FOV_2$.

Because the optimization involves only two scalar parameters, α and SDD_R, a combined solution can be solved for numerically by iterating between marginal solutions until convergence. The algorithm simply chooses an initial $\alpha = \alpha_0$, finds the best corresponding $SDD_R = SDD_{R,0}$ then recalculates the best α and repeats. The results are detailed in Section 5.1.

4. MULTIPLE SOURCE ARRAY SYSTEMS

The secondary objective of this study is to analyze IGCT systems with multiple source arrays in an effort to reduce scan time. The idea is to replicate the entire system so that image acquisition may be done in parallel by two or more sets of detector arrays detecting x-rays from two or more source arrays. Figure 7 illustrates a system with two source arrays, each aimed at their respective set of three detector arrays.

There are two questions to consider: 1) At what angle should the two (or more) source arrays be situated relative to each other? 2) What is the minimum rotation amount of the system to acquire a complete data set to fully reconstruct the volume?

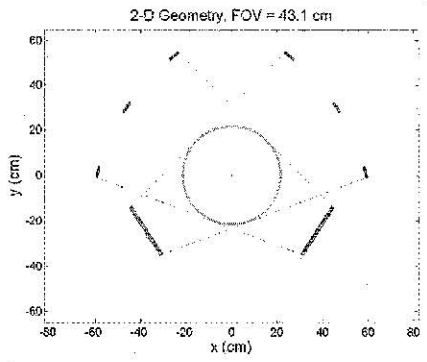

Figure 7. System with two source arrays for parallel acquisition to reduce scan time.

4.1. Partial-scan analysis

Since the objective now is speed of acquisition, we consider the minimum partial-scan rotation angle γ. This is the smallest angle by which the system needs to rotate in order to acquire a complete 180^o data set to fully reconstruct the volume. For a traditional 2-D fan-beam system with a point source and a linear detector, $\gamma = \pi + \phi_{FAN}$ where ϕ_{FAN} is the full fan-angle of the fan-beam system.[3] In our case, the fan-angle is a little ambiguous since neither the source nor the detector is a point. We define the fan-angle for the iGCT system in this analysis (with a single source array) to be $\phi_{FAN} = \theta_{MAX} - \theta_{MIN} = 2\theta_{MAX}$ (due to symmetry), where θ_{MAX} is the Radon angle θ of the ray going from S_R to the left-most detector element of the left detector array (i.e. the most oblique ray angle). We found that the minimum rotation angle is $\gamma \approx \pi + 2\theta_{MAX}$ for a system with one source array.

To see what is happening in Radon space, we make the usual assumption that two opposing rays are equivalent. That is, $(\rho, \theta) = (-\rho, \theta + \pi)$. Figure 8 shows Radon space coverage with this symmetry for a single-source three-detector system. To acquire a full 180^o data set then, a full 360^o range in this symmetric Radon space must be covered. Rotating the gantry by an angle γ is equivalent to a vertical "smearing" of points in Radon space by the same vertical distance γ. So to cover the full space, a rotation of $\gamma \approx \pi + 2\theta_{MAX}$ is necessary.

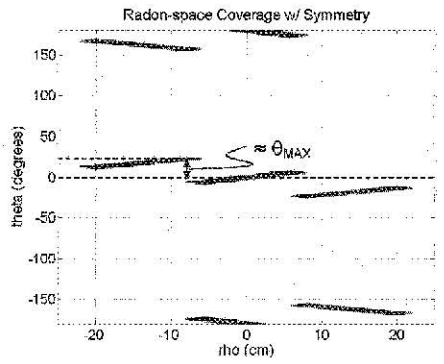

Figure 8. Radon space coverage of a single source array system with the symmetry condition $(\rho, \theta) = (-\rho, \theta + \pi)$. A rotation of $\pi + 2\theta_{MAX}$ is necessary to cover the space completely.

Therefore, for a system with two source arrays, the minimum partial-scan rotation angle is $\gamma_2 = \frac{1}{2}\gamma \approx \frac{\pi}{2} + \theta_{MAX}$ as long as we situate both source arrays to be exactly γ_2 apart. Then as the gantry rotates, each source array (and their corresponding detector arrays) will acquire data from complementary regions in Radon space. This would reduce the total scan time by 50%.

We can imagine an even further reduction in scan time with three source arrays situated $\gamma_3 = \frac{\pi}{3} + \frac{2}{3}\theta_{MAX}$ apart. Unfortunately the system geometry prohibits this due to some source arrays occluding the view of detectors corresponding to other source arrays.

5. RESULTS

5.1. Detector Placement

Iterative joint optimization of the parameters α and SDD_R, characterizing the positions of the detector arrays, was performed. For the fixed system parameters outlined in Table 1 of Section 2.1, the best α and SDD_R were 17.9^o and 113cm, respectively, yielding a FOV of 44cm. The algorithm converged after 3 iterations and because the results show a uniform sampling histogram, we can be sure that it converged to a nearly optimal solution. Figure 9 shows the detector placement and corresponding Radon space coverage and sampling histogram.

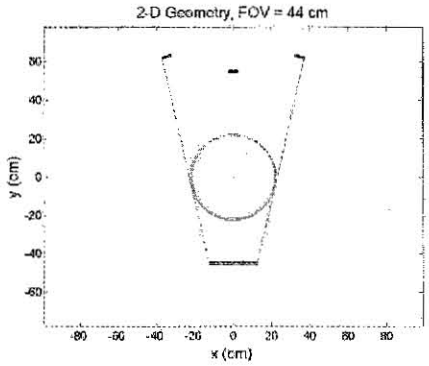

(a) Final optimized system geometry with FOV of 44cm.

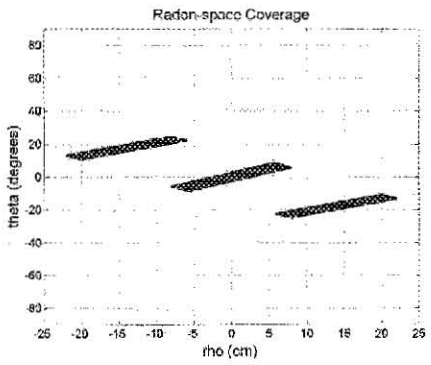

(b) Radon space coverage.

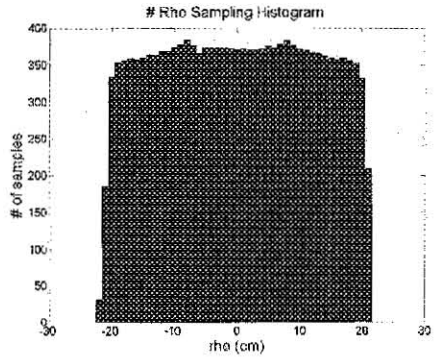

(c) ρ-sampling histogram.

Figure 9. Optimal geometry for fixed $SDD_C = 100$cm.

5.2. Multiple Sources

Three different multiple-source geometries were analyzed, all of them using the FOV-optimized parameters derived in the previous section. The first was a system with two source arrays separated by $\gamma_2 = \frac{\pi}{2} + \theta_{MAX} = 115^o$.

This system has a minimum partial-scan rotation of 115° and a full-scan (360° dataset) minimum rotation of $360 - 115 = 245°$. The other two geometries were both systems with three source arrays. One had a separation between sources of 61° which is the maximum separation allowed due to geometry limitations. The other system had a symmetric spacing of 120° so that the full-scan time was minimized. All three geometries are depicted in Figure 10.

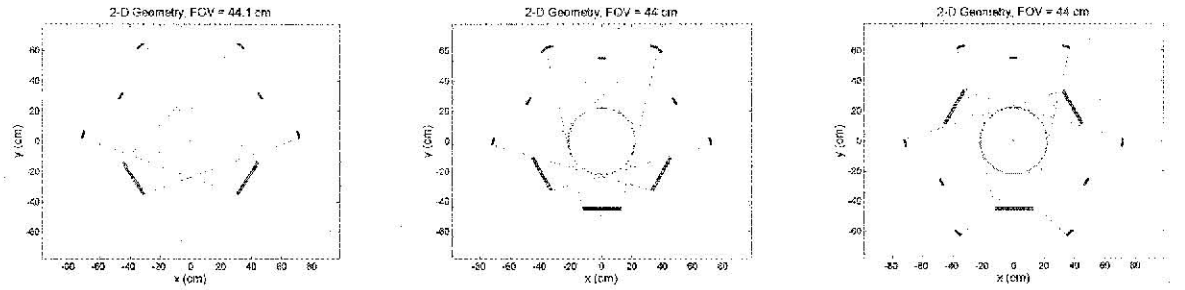

(a) Two source arrays separated by 115°.

(b) Three source arrays separated by 61° (limited by the system geometry).

(c) Three source arrays separated by 120° to minimize the full-scan time.

Figure 10. Three different multi-source systems were analyzed.

Table 2 outlines the results from the geometries considered for multiple source array systems using the FOV-optimized parameters. Note that the rotation angle directly correlates with scan time.

Table 2. Multi-source IGCT system minimum rotation angles.

Number of Source Arrays	Angular Spacing between Sources	Partial-Scan Rotation Angle	Full-Scan Rotation Angle
1	–	229°	360°
2	115°	115°	245°
3	61°	107°	177°
3	120°	120°	120°

6. CONCLUSIONS

In extending the basic single-detector-array IGCT system to a three-detector-array system, we have increased the FOV by three times while maintaining uniform radial sampling of rays. We have also investigated possible multiple source array parallel geometries to reduce the total partial-scan time by 50% of the original partial-scan time using a two-source system and by a little more with a three-source system.

This study focused on maximizing the FOV and minimizing scan time. Other factors such as image resolution, dose efficiency, system complexity, noise, and scatter performance need to be studied. Further multi-parameter optimization is underway.

ACKNOWLEDGMENTS

This work is supported by GE Medical Systems and the Lucas Foundation.

REFERENCES

1. T. Gilat, R. Fahrig, N. Pelc, "Three-dimensional reconstruction algorithm for a reverse geometry volumetric CT system with a large array scanned source," in *Medical Imaging 2003: Physics of Medical Imaging, Proc. SPIE* **5030**, pp. 103-111, 2003.
2. B. D. Smith, "Cone-beam tomography: recent advances and a tutorial review," *Optical Engineering* **29**, pp. 524-534, 1990.
3. C.R. Crawford, K.F. King, "Computed tomography scanning with simultaneous patient translation," *Medical Physics* vol 17, no. 6, pp. 967-982, 1990.